

University of Alabama in Huntsville

LOUIS

---

Honors Capstone Projects and Theses

Honors College

---

4-7-2021

## Investigation of Dusting Hole Film Cooling on a Transonic Turbine Blade Tip With a Squealer

Matthew Cox

Follow this and additional works at: <https://louis.uah.edu/honors-capstones>



Part of the [Heat Transfer, Combustion Commons](#)

---

### Recommended Citation

Cox, Matthew, "Investigation of Dusting Hole Film Cooling on a Transonic Turbine Blade Tip With a Squealer" (2021). *Honors Capstone Projects and Theses*. 268.

<https://louis.uah.edu/honors-capstones/268>

This Thesis is brought to you for free and open access by the Honors College at LOUIS. It has been accepted for inclusion in Honors Capstone Projects and Theses by an authorized administrator of LOUIS.

# Investigation of Dusting Hole Film Cooling on a Transonic Turbine Blade Tip with a Squealer

by

**Matthew Cox**

An Honors Capstone

submitted in partial fulfillment of the requirements

for the Honors Diploma

to

The Honors College

of

The University of Alabama in Huntsville

4/7/2021

Honors Capstone Director: Dr. Phillip Ligrani

Eminent Scholar in Propulsion; Professor of Mechanical and Aerospace Engineering



April 2, 2021

Student

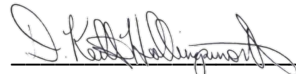
Date



April 2, 2021

Project Advisor

Date



April 8, 2021

Department Chair

Date

Honors College Dean

Date



Honors College  
Frank Franz Hall  
+1 (256) 824-6450 (voice)  
+1 (256) 824-7339 (fax)  
honors@uah.edu

### Honors Thesis Copyright Permission

**This form must be signed by the student and submitted as a bound part of the thesis.**

In presenting this thesis in partial fulfillment of the requirements for Honors Diploma or Certificate from The University of Alabama in Huntsville, I agree that the Library of this University shall make it freely available for inspection. I further agree that permission for extensive copying for scholarly purposes may be granted by my advisor or, in his/her absence, by the Chair of the Department, Director of the Program, or the Dean of the Honors College. It is also understood that due recognition shall be given to me and to The University of Alabama in Huntsville in any scholarly use which may be made of any material in this thesis.

Matthew Cox

Student Name (printed)

Matthew Cox

Student Signature

April 2, 2021

Date

## Abstract

The present study investigates film cooling from a single dusting hole placed in the squealer recess region of a transonic turbine blade with a squealer rim. With no film cooling employed, baseline heat transfer coefficient values are generally higher within the upstream 40 percent of the blade near the leading edge, where heat transfer coefficients are as large as  $2,200 \text{ W/m}^2 \text{ K}$ . The effect of the film cooling from the dusting hole on adiabatic film cooling effectiveness distributions is apparent with locally increased adiabatic effectiveness values around and just downstream of the film cooling hole exit location. In some cases, the heat transfer coefficient ratios are locally decreased, with values as low as 0.60. This is a consequence of reductions in local mixing provided by the film, along with corresponding reductions in the local turbulent transport. Local adiabatic film cooling effectiveness data and heat transfer coefficient data on the squealer blade tip surface are also given along lines. Effectiveness values for line B are especially high with values that vary somewhat with blowing ratio, such that the highest values given for a blowing ratio of 0.64. Adiabatic film cooling effectiveness values are also especially high along line D. The largest local decreases of heat transfer coefficient due to the presence of the film are evident for the D line location, and locally for the B line location.

## Table of Contents

Nomenclature .....	5
List of Figures .....	6
1. Introduction, Experimental Configurations, Apparatus, and Procedures.....	8
2. Experimental Results .....	8
2.1. Baseline Heat Transfer Coefficient Experimental Data.....	8
2.2. Adiabatic Film Cooling Effectiveness Experimental Data .....	9
2.3. Heat Transfer Coefficient and Heat Transfer Coefficient Ratio Experimental Data .....	9
3. Summary and Conclusions .....	11
References .....	24

## **Nomenclature**

$\eta_{ad}$  = adiabatic film cooling effectiveness

BR = film cooling blowing ratio

$C_x$  = blade chord length

h = heat transfer coefficient

$h_0$  = baseline heat transfer coefficient

x = streamwise coordinate

y = spanwise coordinate

## List of Figures

Figure 1: Blade A1 film cooling hole locations. ....	13
Figure 2: Blade A1 tip thermocouple locations.....	14
Figure 3: Heat transfer coefficient $c_0$ baseline data with BR = 0 and 1.4 mm tip gap. ....	14
Figure 4: Scale 0 to 0.5 for adiabatic film cooling effectiveness $c_{21}$ data with BR = 2.49 and 1.4 mm tip gap. ....	15
Figure 5: Scale 0 to 1 for adiabatic film cooling effectiveness $c_{21}$ data with BR = 2.49 and 1.4 mm tip gap. ....	15
Figure 6: Heat transfer coefficient $c_{21}$ data with BR = 2.49 and 1.4 mm tip gap. ....	16
Figure 7: Heat transfer coefficient ratio $c_{21}$ data with BR = 2.49 and 1.4 mm tip gap. ....	16
Figure 8: Line plot for adiabatic film cooling effectiveness $c_{15}$ data with BR = 1.58 and 1.4 mm tip gap. ....	17
Figure 9: Blade A1 adiabatic film cooling effectiveness, line A. ....	17
Figure 10: Blade A1 adiabatic film cooling effectiveness, line B. ....	18
Figure 11: Blade A1 adiabatic film cooling effectiveness, line C. ....	18
Figure 12: Blade A1 adiabatic film cooling effectiveness, line D. ....	19
Figure 13: Heat transfer coefficient line plot $c_{15}$ data with BR = 1.58 and 1.4 mm tip gap. ....	19
Figure 14: Blade A1 heat transfer coefficient ratio, line A. ....	20
Figure 15: Blade A1 heat transfer coefficient ratio, line B. ....	20
Figure 16: Blade A1 heat transfer coefficient ratio, line C. ....	21
Figure 17: Blade A1 heat transfer coefficient ratio, line D. ....	21
Figure 18: Location of area-averaged adiabatic film cooling effectiveness $c_{15}$ data with BR = 1.58 and 1.4 mm tip gap. ....	22
Figure 19: Blade A1 adiabatic film cooling effectiveness variation with blowing ratio BR. ....	22
Figure 20: Location of area-averaged HTC ratio data for $c_{15}$ with BR = 1.58 and 1.4 mm tip gap. ....	23

Figure 21: Blade A1 heat transfer coefficient ratio variation with blowing ratio BR. .... 23



## **1. Introduction, Experimental Configurations, Apparatus, and Procedures**

The present study investigates film cooling from a single dusting hole placed in the squealer recess region of a transonic turbine blade with a squealer rim. Different blowing ratios are considered for the dusting hole. The experimental apparatus and details on the experimental configuration are provided by Collopy [1]. The cascade configuration, film cooling supply apparatus, turbine blade configuration, and turbine blade tip configuration are also provided by Collopy [1]. In Figure 1, the film cooling dusting hole location is shown, including the  $x$  millimeter location and the  $x/C_x$  location. Figure 2 then shows the thermocouple locations used for calibration of the infrared camera during transient, transonic testing. Locations of the thermocouple and the thermocouple inserts are shown in a table which is included Figure 2. For additional information on experimental apparatus, procedures, and configuration details, the reader is referred to Collopy [1].

## **2. Experimental Results**

### **2.1. Baseline Heat Transfer Coefficient Experimental Data**

Figure 3 shows dimensional, baseline heat transfer coefficient data for the transonic blade tip, with a squealer, and no film cooling employed. These data are provided as they vary with  $y/C_x$  and  $x/C_x$  to show surface variations along the blade tip, relative to the locations of the squealer rims and squealer recess. Within Figure 3, the pressure side is on the left side of the blade and the suction side is on the right side of the blade. The leading edge is toward the top of the blade and the trailing edge is toward the bottom of the blade. Note that not all of the data on the trailing edge are shown because of the view employed by the infrared camera to acquire the data. Generally, heat transfer coefficient values are higher within the upstream 40 percent of the blade near the leading edge, where heat transfer coefficients are as high as 2,200  $W/m^2 K$ . Heat transfer coefficients that are significantly lower are apparent along the downstream portion of the blade. Also apparent are significantly different variations within the squealer recess region, near the

suction side rim and the pressure side rim. The lowest local values are apparent along the suction side rim from  $x/Cx$  from 0.40 to 0.75.

## **2.2. Local Adiabatic Film Cooling Effectiveness Experimental Data**

Figure 4 shows local adiabatic film cooling effectiveness data. These data are given for the c21 film cooling carbon dioxide injection arrangement with a blowing ratio of 2.49. All data are provided for a 1.4 mm tip gap. The data in Figure 4 are given for a maximum adiabatic film cooling effectiveness scale of 0.5. The data in Figure 5 are the same data but they are given for a maximum adiabatic film cooling effectiveness scale of 1.0. The effect of the film cooling from the dusting hole on these distributions is apparent with locally increased adiabatic effectiveness values around and just downstream of the film cooling hole exit location. Also apparent in Figures 4 and 5 are augmented effectiveness regions, along the suction side squealer rim, at locations which are downstream of the dusting hole exit location.

## **2.3. Heat Transfer Coefficient and Heat Transfer Coefficient Ratio Experimental Data**

Surface heat transfer coefficient data for the c21 film cooling condition with a blowing ratio of 2.49 and a 1.4 mm tip gap are shown in Figure 6. The corresponding heat transfer coefficient ratio data are then shown in Figure 7. Pronounced variations are apparent along the blade tip surface because of the presence of the film. In some cases, the heat transfer coefficient ratios are locally decreased, with values as low as 0.60. This is a consequence of reductions in local mixing provided by the film, along with corresponding reductions in the local turbulent transport. Local heat transfer coefficient ratio increases are evident near the leading edge of the film concentration, which evidence augmented local mixing, as a result of the presence of a horseshoe vortex. Here, heat transfer coefficient ratios are as high as 1.40.

## **2.4. Adiabatic Film Cooling Effectiveness Experimental Data - Line Variations**

Local adiabatic film cooling effectiveness data on the squealer blade tip surface are also given along lines. These lines are labelled A, B, C, and D, and are shown in Figure 8. Effectiveness variations along line A are shown in Figure 9, variations along line B are shown in Figure 10, variations along line C are

shown in Figure 11, and variations along line D are shown in Figure 12. Note that the  $x/C_x$  and  $y/C_x$  coordinates within these figures match the  $x/C_x$  and  $y/C_x$  coordinates shown in Figure 8. These data are shown for different C-values, which correspond to different blowing ratio values, where the relationship between blowing ratio and C-values is given in Table 1. The vertical lines within these figures are the locations of the squealer rims, both near the pressure side or the suction side of the blade tip surface. Figure 10 shows that effectiveness values for line B are especially high with values that vary somewhat with blowing ratio, such that the highest values given for a blowing ratio of 0.64. Figure 12 shows that adiabatic film cooling effectiveness values are also especially high along line D. For lines C and D, in some cases, local film cooling effectiveness increases with blowing ratio, and in other cases, film cooling effectiveness decreases as blowing ratio increases.

## **2.5. Heat Transfer Coefficient and Heat Transfer Coefficient Ratio Experimental Data - Line Variations**

Local heat transfer coefficient ratio data on the squealer blade tip surface are also given along lines. These lines are labelled A, B, C, and D, and are shown in Figure 13. Effectiveness variations along line A are shown in Figure 14, variations along line B are shown in Figure 15, variations along line C are shown in Figure 16, and variations along line D are shown in Figure 17. In many cases, local heat transfer coefficient ratio variations are quite complex. The largest local decreases due to the presence of the film are evident in Figure 17 for the D line location, and locally in Figure 15 for the B line location. Overall, the data in Figures 14, 15, 16, and 17 show that, for some locations and conditions, heat transfer coefficient ratios increase as blowing ratio increases, and for other locations and conditions, heat transfer coefficient ratios increase as blowing ratio decreases.

## **2.6. Adiabatic Film Cooling Effectiveness Experimental Data - Area-Averaged Variations**

Locations for area-averaged adiabatic film cooling effectiveness data are given in Figure 18. The data in Figure 18 are given for a c15 condition, blowing ratio of 1.58, and tip gap of 1.4 mm. Corresponding

area-averaged results are shown in Figure 19. Important variations are evident within the squealer recess region, where values are as high as 0.8. Pressure side squealer rim values are near zero. Suction side squealer rim values are near zero for lower blowing ratios, but increase to values near 0.25 for higher blowing ratios.

### **2.7. Heat Transfer Coefficient and Heat Transfer Coefficient Ratio Experimental Data - Area-Averaged Variations**

Locations for area-averaged heat transfer coefficient ratio data are given in Figure 20. The data in Figure 20 are given for a c15 condition, blowing ratio of 1.58, and tip gap of 1.4 mm. Corresponding area-averaged results are shown in Figure 21. For the data on the pressure side squealer rim, values are near 1.0. For the data on the suction side squealer rim, values are slightly greater than 1.0 for blowing ratios less than 2.0, and are somewhat less than 1.0 for blowing ratios greater than 2.0. For the squealer recess region, values are less than 1.0 for all blowing ratios considered.

### **3. Summary and Conclusions**

The present study investigates film cooling from a single dusting hole placed in the squealer recess region of a transonic turbine blade with a squealer rim. Local, spatially-varying adiabatic film cooling effectiveness data show that the effect of the dusting hole is locally increased adiabatic effectiveness values around and just downstream of the film cooling hole exit location. Surface heat transfer coefficient ratio data for a blowing ratio of 2.49 and a 1.4 mm tip gap illustrate pronounced variations along the blade tip surface because of the presence of the film. In some cases, the heat transfer coefficient ratios are locally decreased, with values as low as 0.60. This is a consequence of reductions in local mixing provided by the film, along with corresponding reductions in the local turbulent transport.

Local adiabatic film cooling effectiveness data show that effectiveness values for line B are especially high with values that vary somewhat with blowing ratio, such that the highest values given for a blowing ratio of 0.64. Local adiabatic film cooling effectiveness values are also especially high along line D. Local

heat transfer coefficient ratio data on the squealer blade tip surface show that the largest local decreases due to the presence of the film are evident for the D line location, and locally for the B line location.

Area-averaged adiabatic film cooling effectiveness data show important variations within the squealer recess region, where values are as high as 0.8. Pressure side squealer rim values are near zero. Suction side squealer rim values are near zero for lower blowing ratios, but increase to values near 0.25 for higher blowing ratios. Area-averaged heat transfer coefficient ratio data show that results for the pressure side squealer rim are near 1.0. For the data on the suction side squealer rim, values are slightly greater than 1.0 for blowing ratios less than 2.0 and are somewhat less than 1.0 for blowing ratios greater than 2.0. For the squealer recess region, values are less than 1.0 for all blowing ratios considered.

Table 1: CO2 injection arrangements and corresponding blowing ratios.

CO2 Injection Arrangement	BR
c11	0.64
c13	1.18
c15	1.58
c18	2.11
c21	2.49
c23	2.94

Film Cooling		
No.	x (mm)	x/Cx
1	14.970	0.206

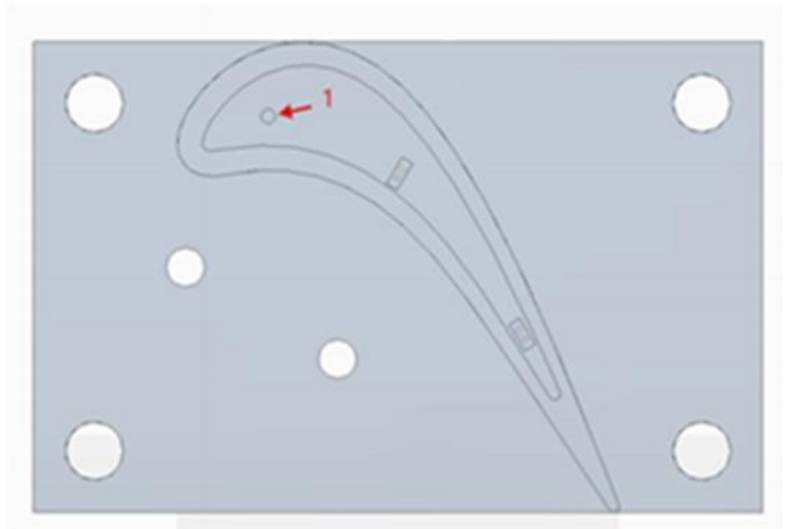


Figure 1: Blade A1 film cooling hole locations.

Thermocouple Inserts		
No.	x (mm)	x/Cx
1	36.170	0.498
2	56.341	0.775
3	57.199	0.787
4	37.024	0.509

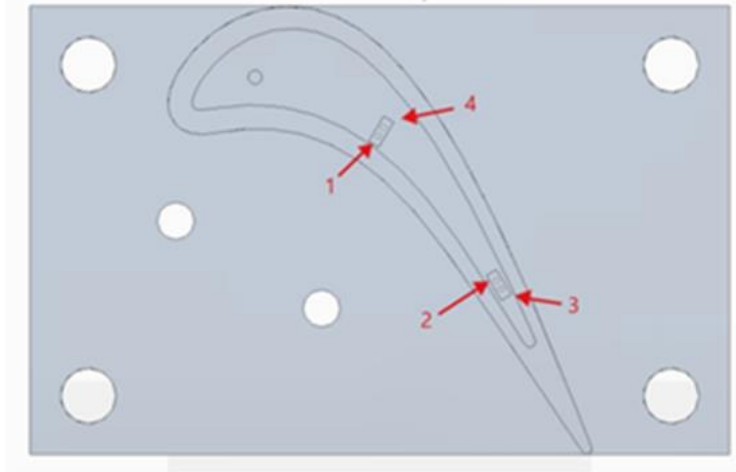


Figure 2: Blade A1 tip thermocouple locations.

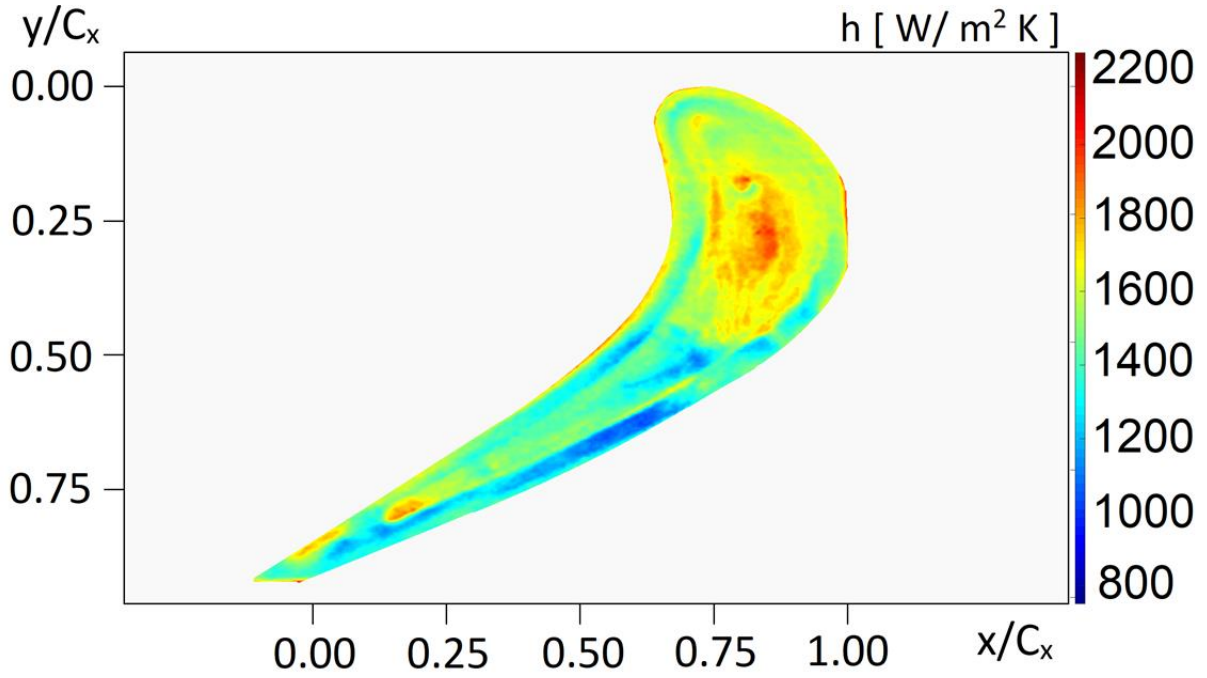


Figure 3: Heat transfer coefficient  $c_0$  baseline data with  $BR = 0$  and 1.4 mm tip gap.

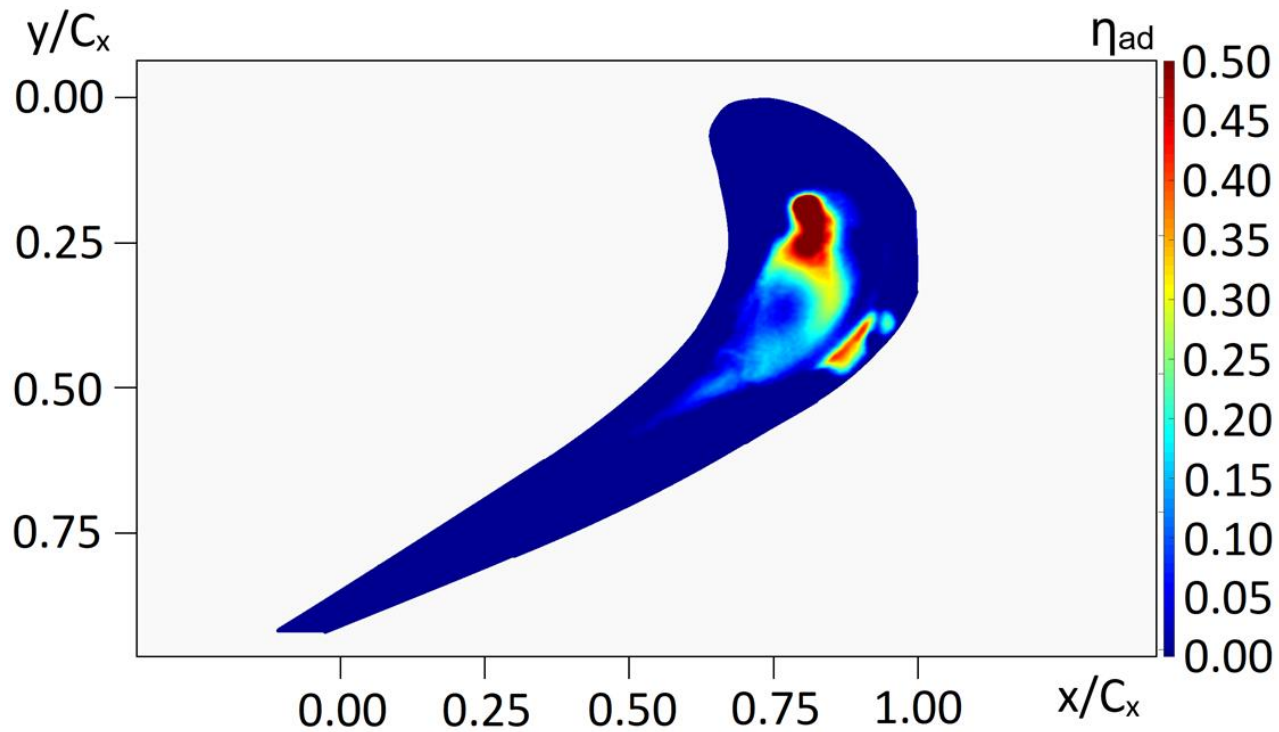


Figure 4: Scale 0 to 0.5 for adiabatic film cooling effectiveness  $c_{21}$  data with  $BR = 2.49$  and 1.4 mm tip gap.

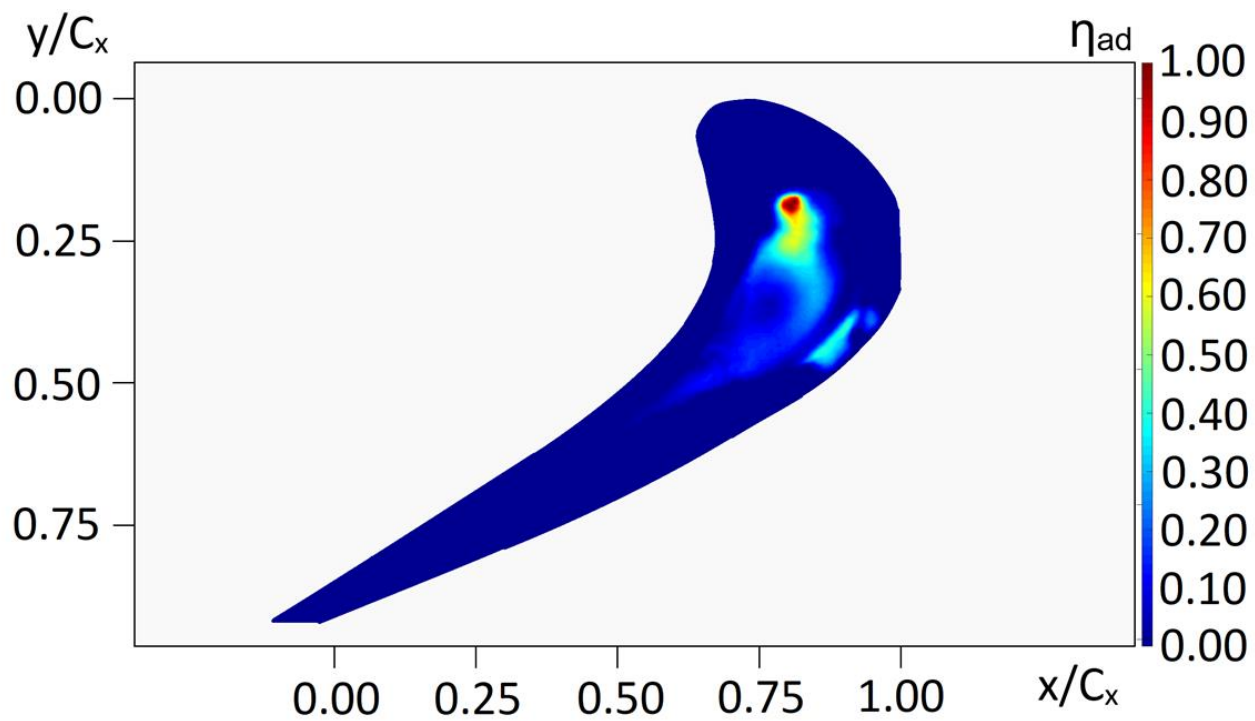


Figure 5: Scale 0 to 1 for adiabatic film cooling effectiveness  $c_{21}$  data with  $BR = 2.49$  and 1.4 mm tip gap.



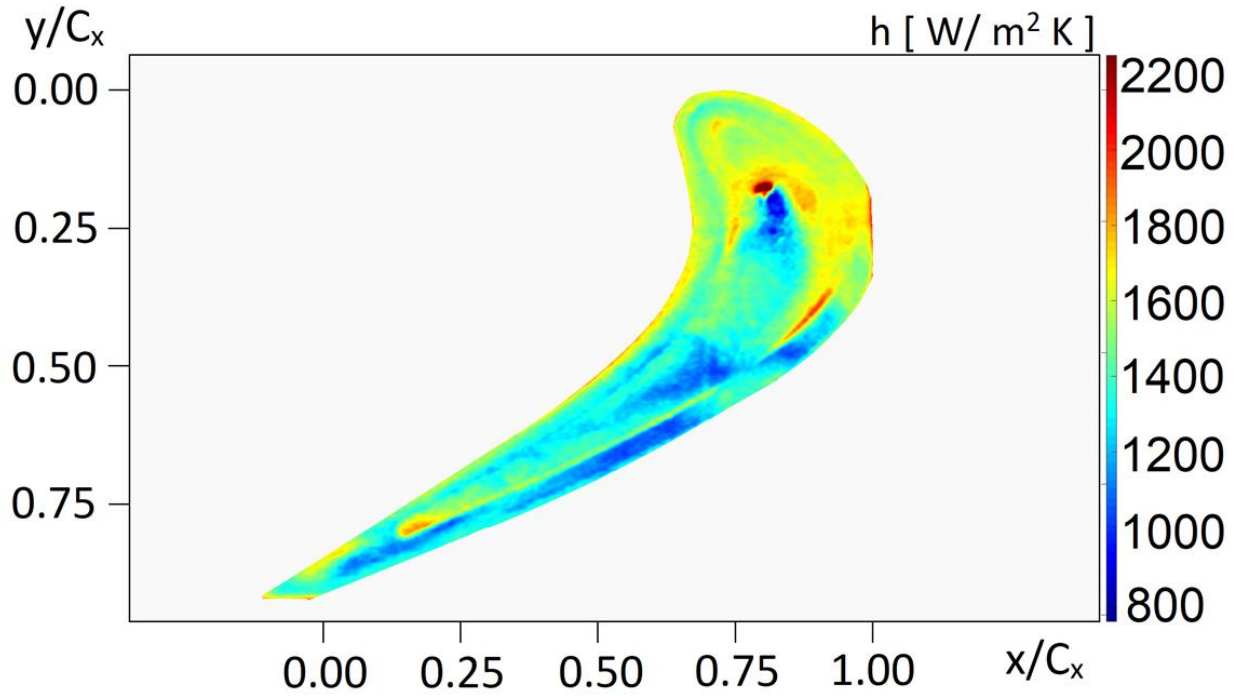


Figure 6: Heat transfer coefficient  $c_{21}$  data with  $BR = 2.49$  and 1.4 mm tip gap.

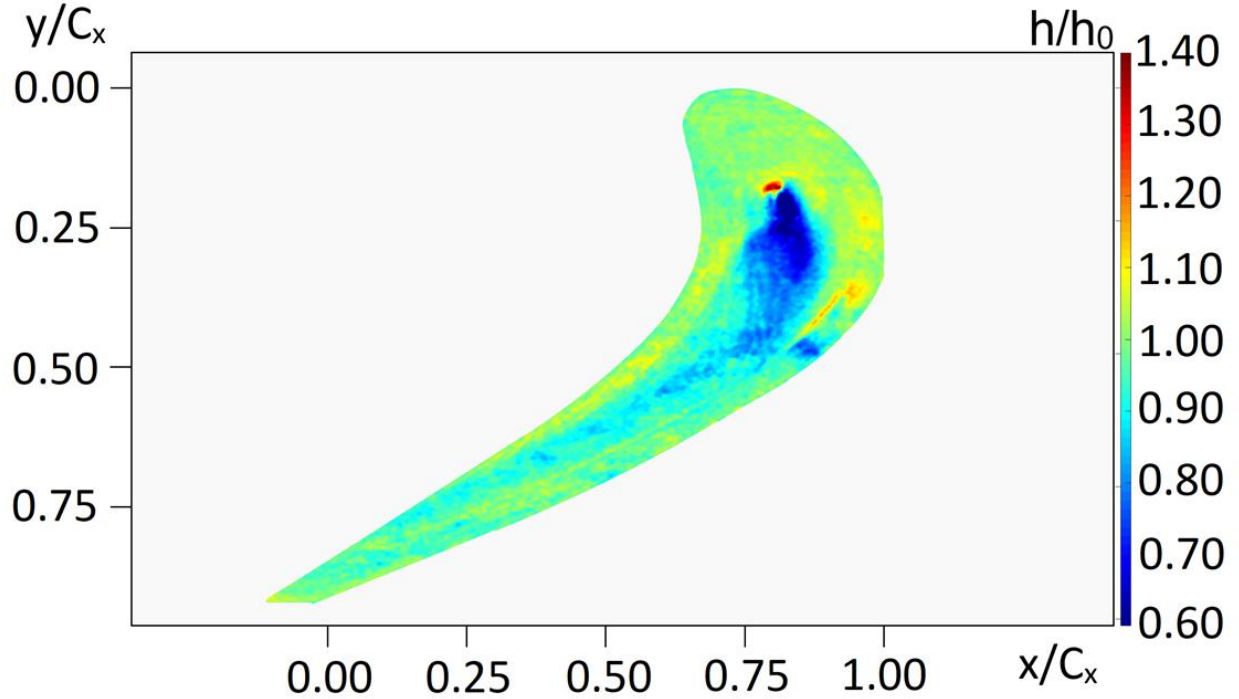


Figure 7: Heat transfer coefficient ratio  $c_{21}$  data with  $BR = 2.49$  and 1.4 mm tip gap.

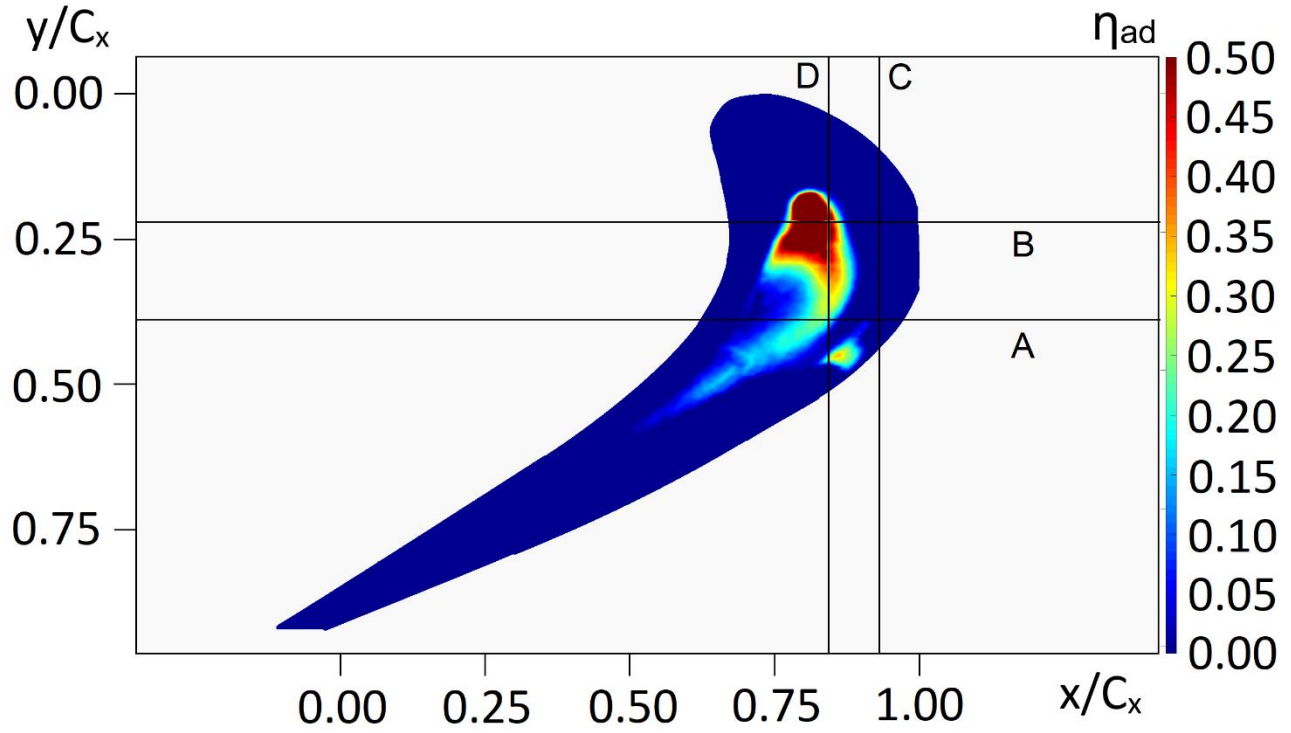


Figure 8: Line plot for adiabatic film cooling effectiveness c15 data with BR = 1.58 and 1.4 mm tip gap.

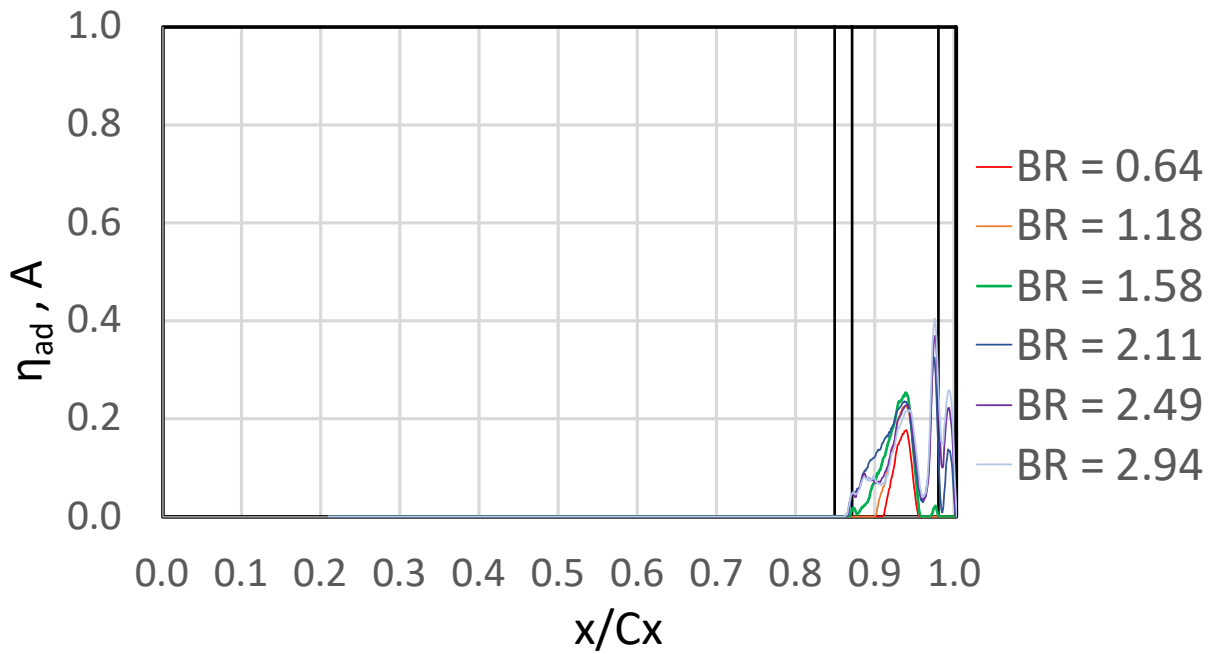


Figure 9: Blade A1 adiabatic film cooling effectiveness, line A.

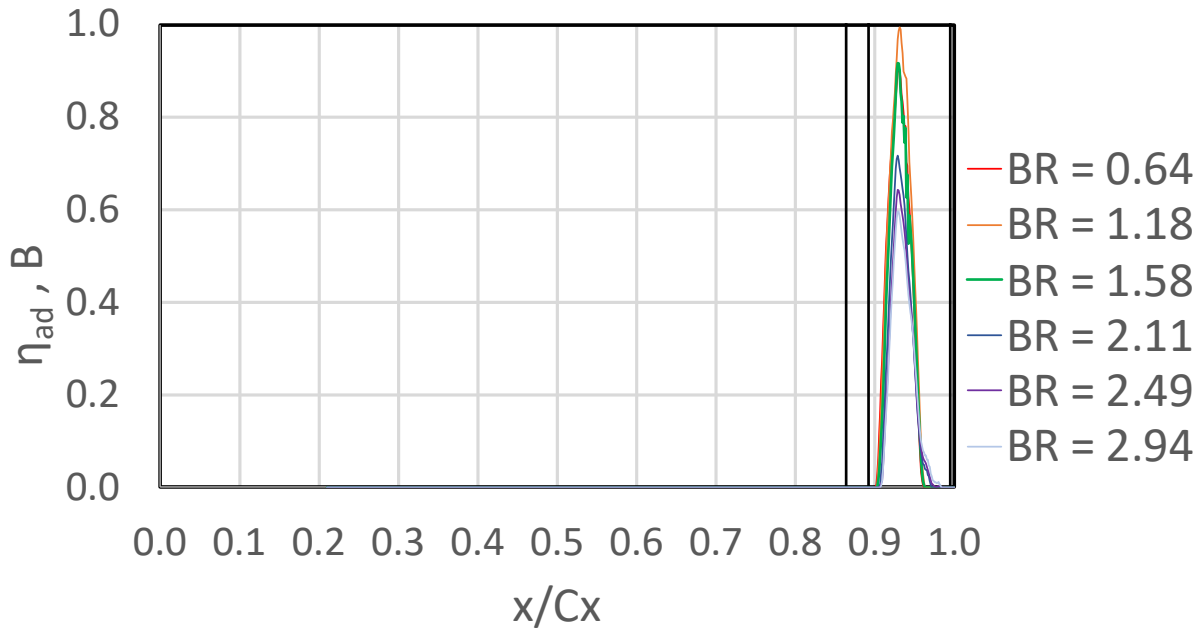


Figure 10: Blade A1 adiabatic film cooling effectiveness, line B.

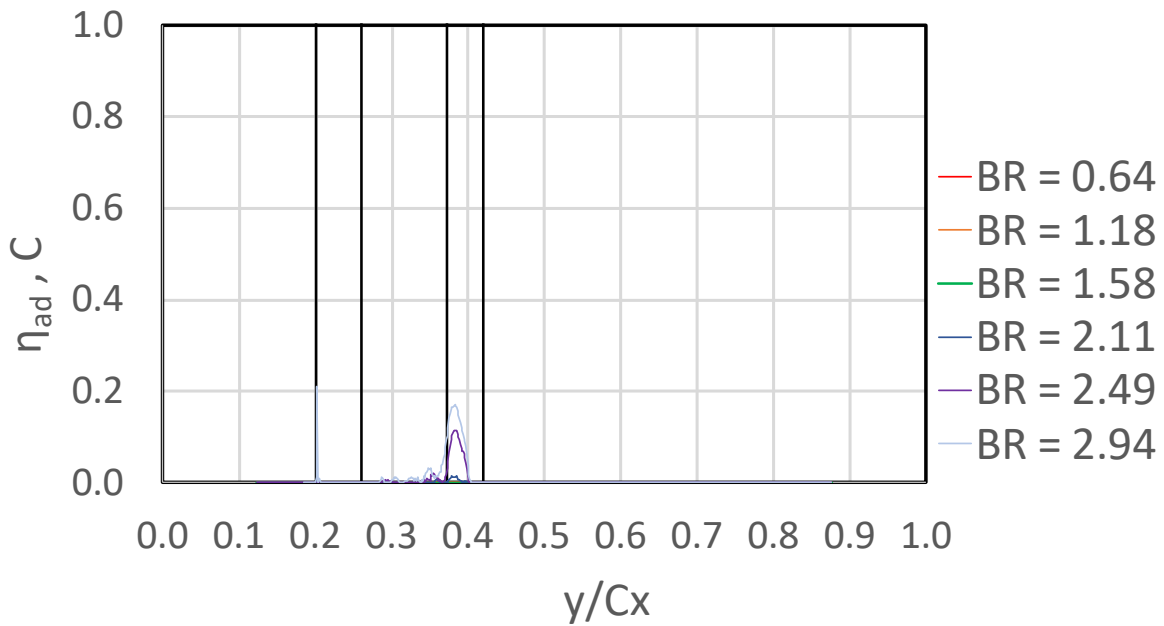


Figure 11: Blade A1 adiabatic film cooling effectiveness, line C.

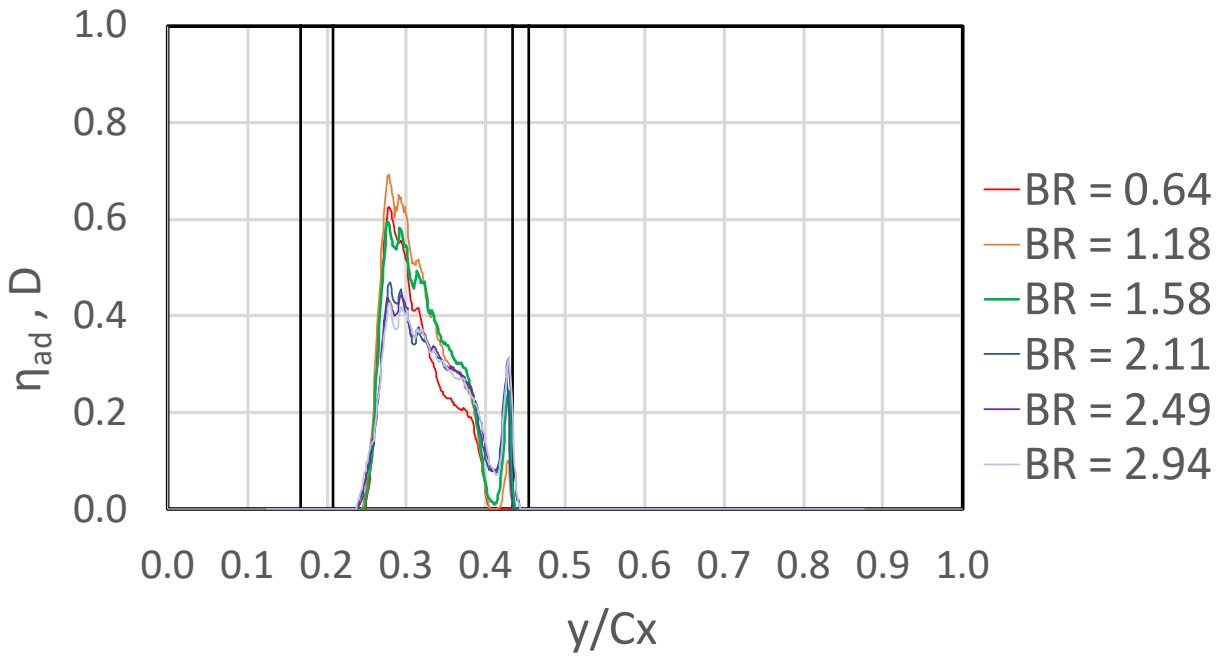


Figure 12: Blade A1 adiabatic film cooling effectiveness, line D.

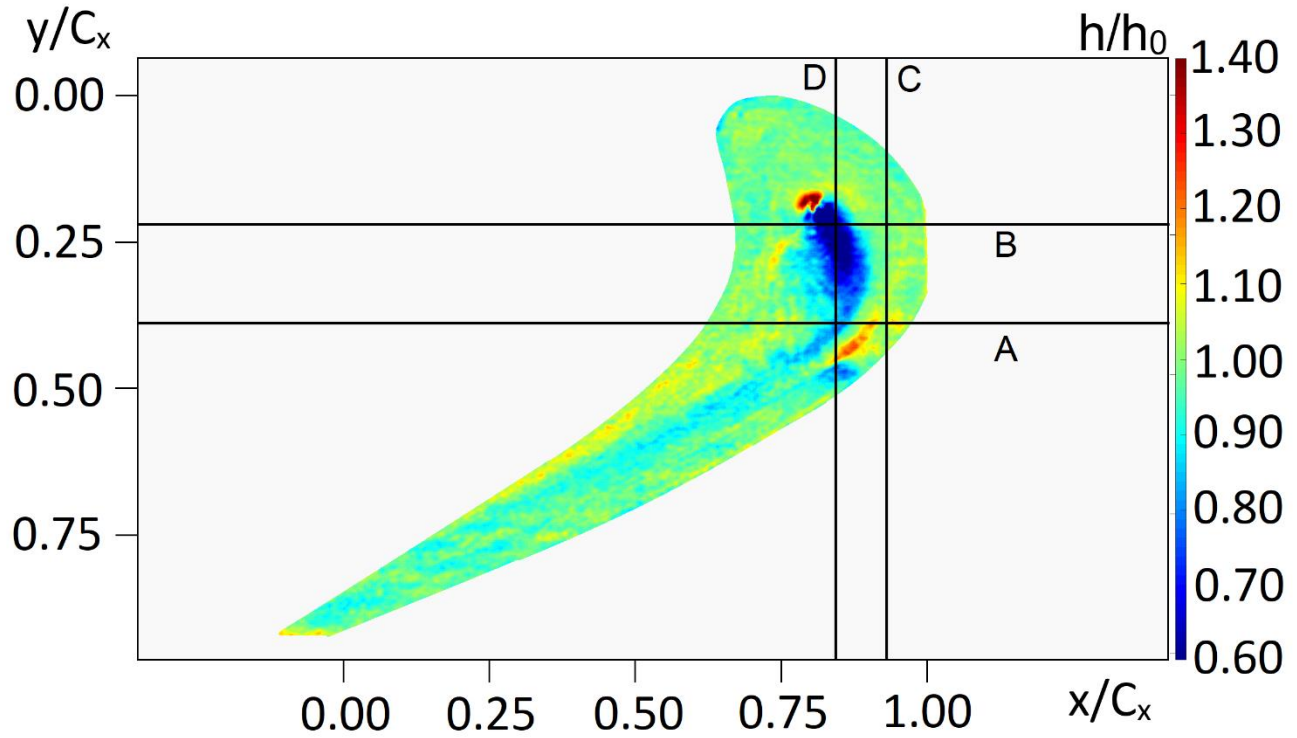


Figure 13: Heat transfer coefficient line plot c15 data with  $BR = 1.58$  and 1.4 mm tip gap.

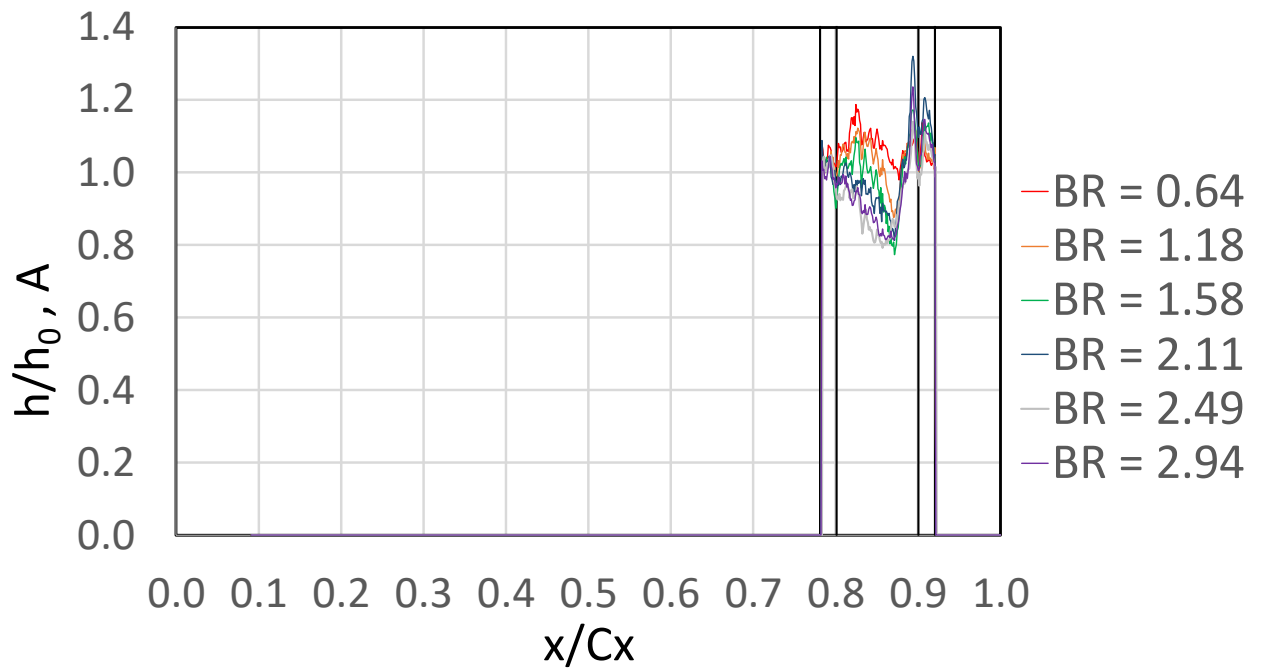


Figure 14: Blade A1 heat transfer coefficient ratio, line A.

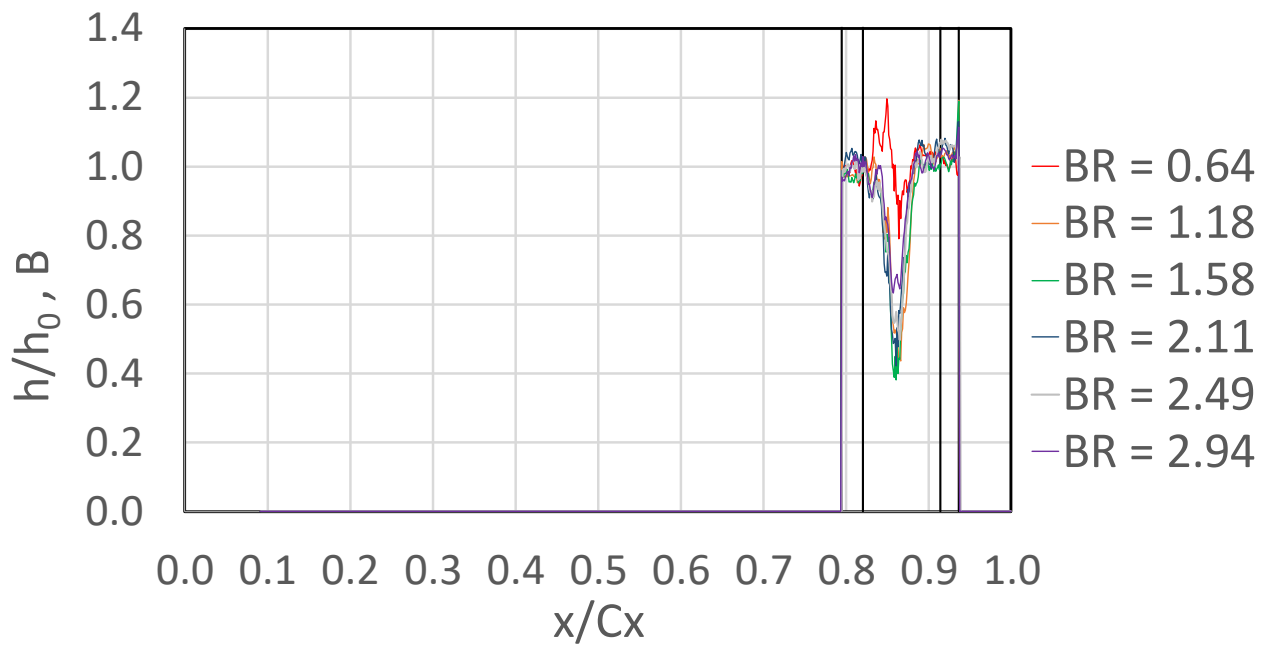


Figure 15: Blade A1 heat transfer coefficient ratio, line B.

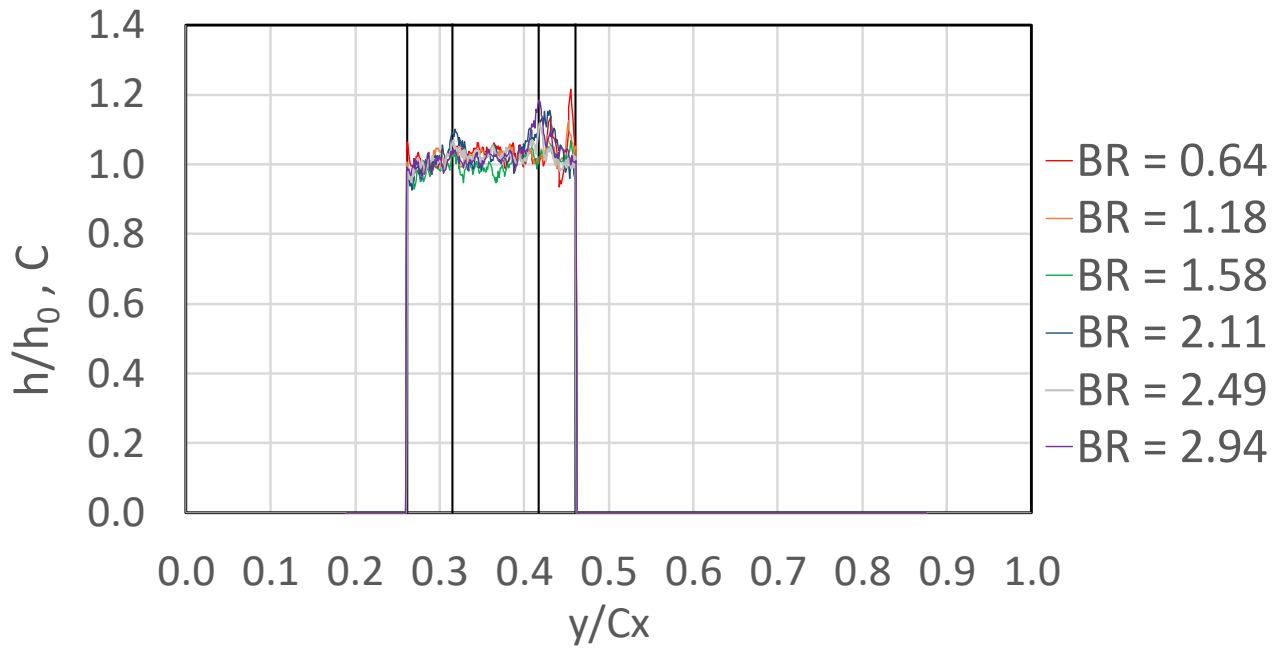


Figure 16: Blade A1 heat transfer coefficient ratio, line C.

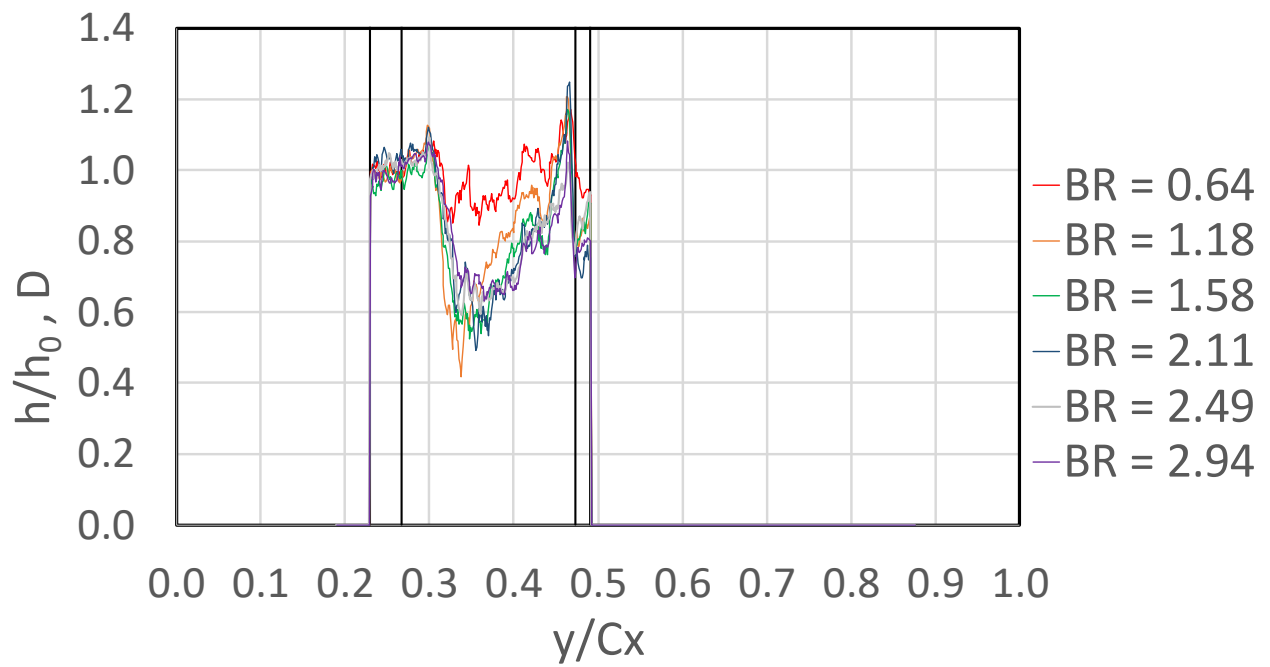


Figure 17: Blade A1 heat transfer coefficient ratio, line D.

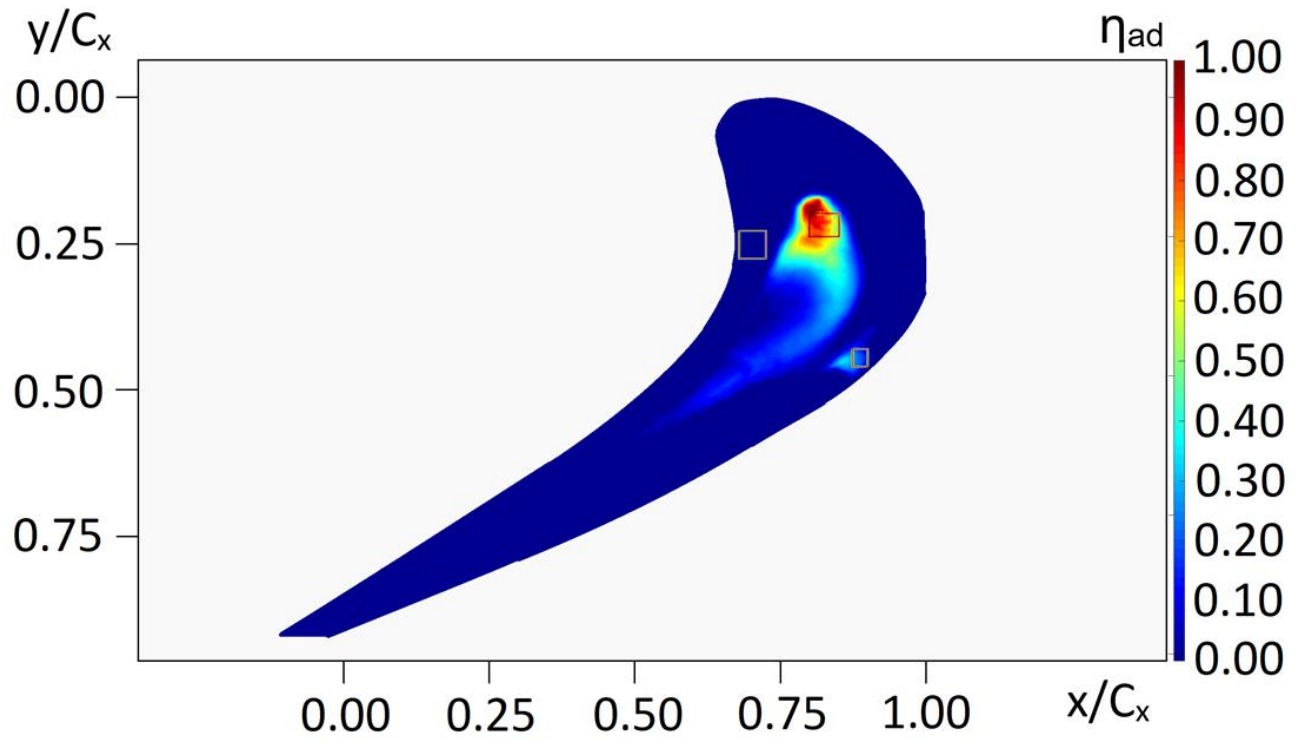


Figure 18: Location of area-averaged adiabatic film cooling effectiveness  $c_{15}$  data with  $BR = 1.58$  and  $1.4$  mm tip gap.

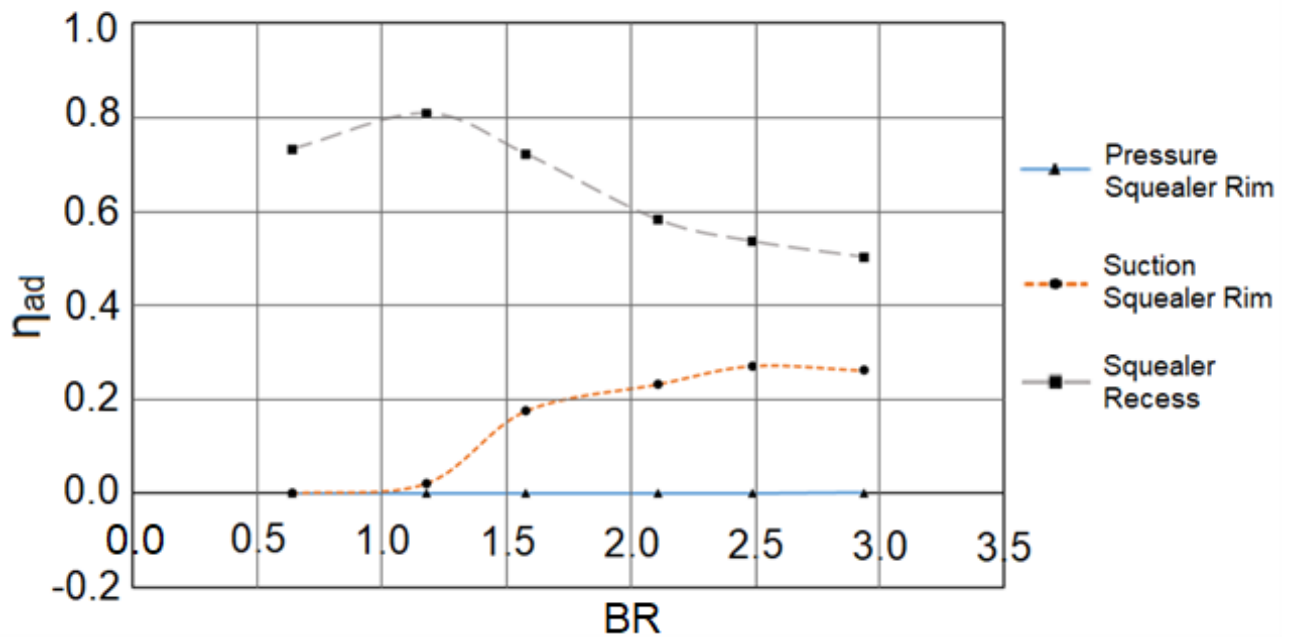


Figure 19: Blade A1 adiabatic film cooling effectiveness variation with blowing ratio  $BR$ .

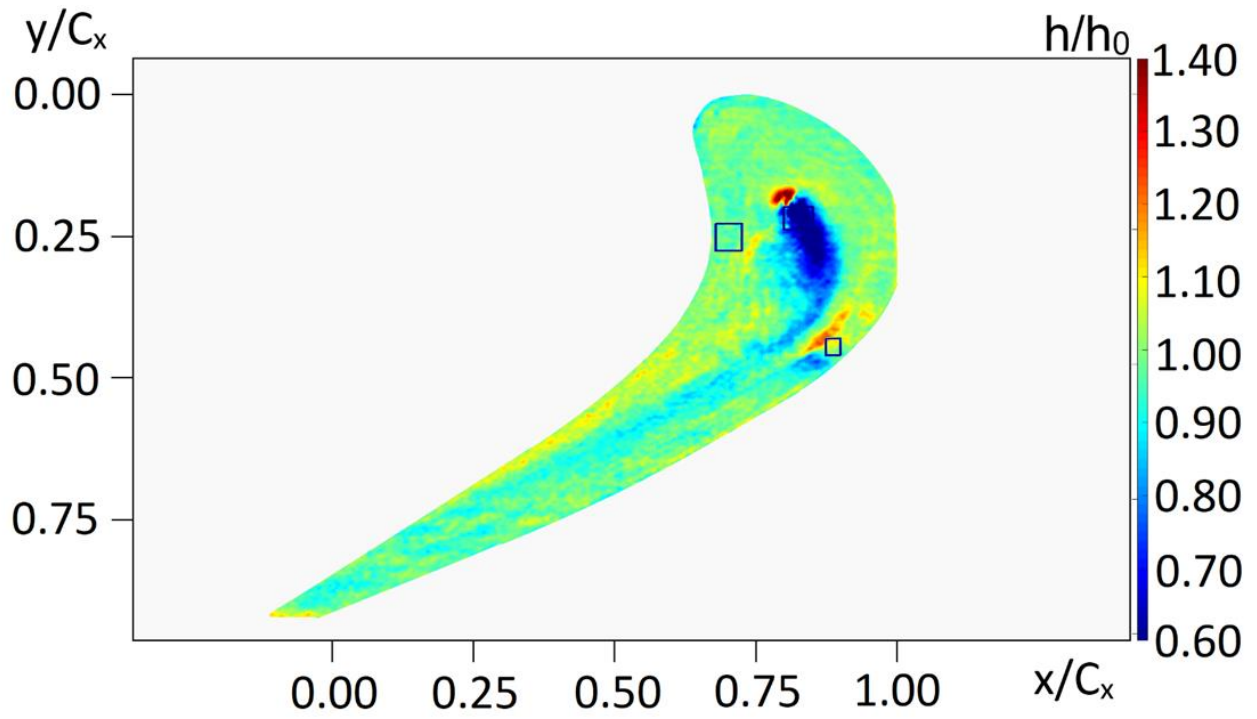


Figure 20: Location of area-averaged HTC ratio data for c15 with BR = 1.58 and 1.4 mm tip gap.

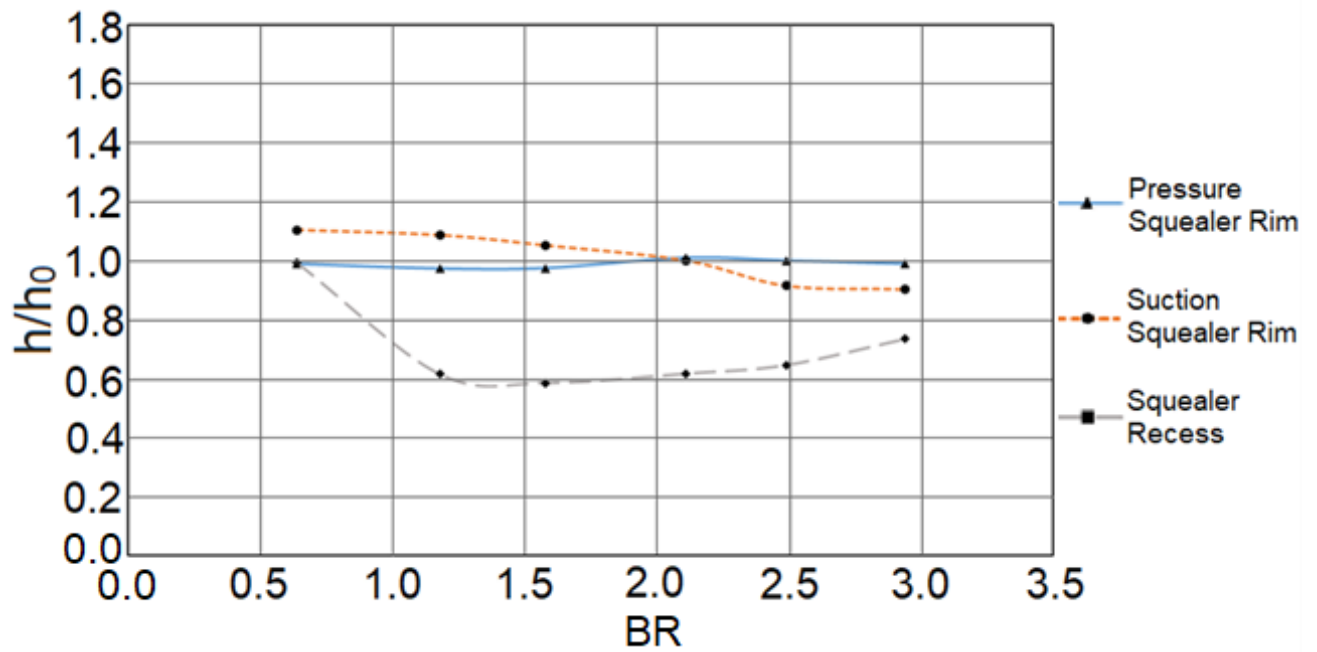


Figure 21: Blade A1 heat transfer coefficient ratio variation with blowing ratio BR.



## References

- [1] H. Collopy, "Surface Heat Transfer Characteristics of A Transonic Turbine Blade With Pressure Side Film Cooling And Different Tip Gaps," Master of Science Thesis, Department of Mechanical and Aerospace Engineering, University of Alabama in Huntsville, Huntsville, Alabama, USA 2020.